Simplified optical quantum-information processing via weak cross-Kerr nonlinearities

Qi Guo,[1] Juan Bai,[1] Liu-Yong Cheng,[1] Xiao-Qiang Shao,[2] Hong-Fu Wang,[1] and Shou Zhang[1,*]

[1]*Department of Physics, College of Science, Yanbian University, Yanji, Jilin 133002, People's Republic of China*

[2]*Center for the Condensed-Matter Science and Technology, Department of Physics, Harbin Institute of Technology, Harbin, Heilongjiang 150001, People's Republic of China*

(Received 7 January 2011; revised manuscript received 22 March 2011; published 23 May 2011)

We propose a simplified parity meter for photonic qubits with cross-Kerr nonlinearities, homodyne measurement, and some optical elements. Our scheme has lower error probability than the protocol proposed in Nemoto and Munro [Phys. Rev. Lett. **93**, 250502 (2004)]. Based on the present parity meter, we achieve cluster-state preparation, a complete Bell-state analyzer, and quantum teleportation. All of these schemes are nearly deterministic in the regime with little noise and include less optical elements, which makes our schemes more meaningful for large-scale quantum computing.

DOI: 10.1103/PhysRevA.83.054303 PACS number(s): 03.67.−a, 42.50.Ex, 42.65.−k

In recent years, quantum-information processing (QIP) has been investigated quite extensively and deeply. Many schemes for QIP have been proposed in different quantum systems, such as cavity QED [1,2], trapped-ion systems [3,4], quantum-dot systems [5,6], superconducting quantum systems [7,8], and linear optical systems [9,10]. In 2001, Knill, Laflamme, and Milburn (KLM) [9] proposed that measurements can provide the means to implement a controlled-NOT (CNOT) gate on boson qubits using single photon sources, detectors, and linear elements. This pioneering work opened the gate of measurement-based quantum computation. Thereafter, many approaches for QIP based on measurement were proposed in both boson systems [11–13] and fermion systems [14–20]. However, because of the probabilistic nature of gates in linear optical QIP, it is difficult to achieve deterministic QIP using only single-photon sources and linear optical elements, including feedforward. In 2003, Munro *et al.* [21] induced an interaction between the photons, which moved optical QIP beyond linear optics and brought the hope of deterministic optical QIP. This interaction is achieved by using a cross-Kerr nonlinear medium. Strong Kerr nonlinearities are difficult to achieve in experiment, so their later works [22–25] used strong coherent state and weak cross-Kerr nonlinearities generated with electromagnetically induced transparencies to realize nearly deterministic quantum gates. Recently, more and more attention [26–28] has been given to optical QIP with weak cross-Kerr nonlinearities.

In general, cross-Kerr nonlinearities can be described with the Hamiltonian as [21–23] $\hat{H} = \hbar\chi\hat{n}_a\hat{n}_c$, where $\hat{n}_a$ and $\hat{n}_c$ are the photon number operators for modes a and c, respectively. χ is the coupling strength of the nonlinearity, and it is decided by the property of the nonlinear material. We consider the signal mode a to be a Fock state $|n_a\rangle$ containing n_a photons and the probe mode c to be a coherent state $|\alpha_c\rangle$ with amplitude α_c. The cross-Kerr nonlinearity causes the combined system of the two modes to evolve as $e^{i\chi t\hat{n}_a\hat{n}_c}|n_a\rangle|\alpha_c\rangle = |n_a\rangle|\alpha_c e^{in_a\theta}\rangle$, where $\theta = \chi t$ and t is the interaction time. It is clear that the phase shift picked up by the coherent state is directly proportional to the number of photons in signal mode a and that the Fock state is unaffected. So the measurement on the phase of probe beam can distinguish the photon numbers in signal mode.

In this Brief Report, first, we simplify the parity meter in Ref. [23] and discuss the advantages of the simplification. Then, we investigate the applications of the present parity meter in the optical QIP, including cluster-state preparation, a complete Bell-state analyzer (BSA), and a scheme for deterministic quantum teleportation. Finally, discussions and a summary are given.

Based on the qubit-parity meter presented in Ref. [23], we first proposed a simpler qubit-parity meter, as shown in Fig. 1. Compared with the former one, our device is an effective simplification by removing two polarizing beam splitters (PBS) and several mirrors (not shown). This simplification is meaningful for large-scale quantum computing. Furthermore, we will demonstrate that the present scheme has a lower error rate than in Ref. [23].

Assume two polarization photons with the form

$$|\psi_1\rangle = \alpha|H\rangle + \beta|V\rangle, \quad |\psi_2\rangle = \delta|H\rangle + \gamma|V\rangle, \tag{1}$$

where $|\alpha|^2 + |\beta|^2 = |\delta|^2 + |\gamma|^2 = 1$. The probe beam is the coherent state $|\alpha_c\rangle$. After passing through the first PBS, there is only one photon in each spatial mode (called balanced) for the initial state $|H\rangle_1|H\rangle_2$ or $|V\rangle_1|V\rangle_2$, while there is zero or two photons in each spatial mode (called bunched) for the initial state $|H\rangle_1|V\rangle_2$ or $|V\rangle_1|H\rangle_2$. Then, the photons interact with two separate weak cross-Kerr nonlinearities, as shown in Fig. 1. The subsequent PBS is used to separate two photons into different spatial modes. Therefore, after the PBSs and cross-Kerr nonlinearities, the joint state will evolve into

$$\begin{aligned}|\psi_{12\alpha_c}\rangle = {} & (\alpha\delta|HH\rangle + \beta\gamma|VV\rangle)|\alpha_c\rangle + (\alpha\gamma|HV\rangle|\alpha_c e^{-i2\theta}\rangle \\ & + \beta\delta|VH\rangle|\alpha_c e^{i2\theta}\rangle).\end{aligned} \tag{2}$$

Obviously, the probe beam receives no phase for the $|H\rangle_1|H\rangle_2$ and $|V\rangle_1|V\rangle_2$ components of the state, while the probe mode receives -2θ and $+2\theta$ phase shifts for the $|H\rangle_1|V\rangle_2$ and $|V\rangle_1|H\rangle_2$ components, respectively. Now we have to perform an X homodyne measurement [23] to obtain the projection of

*szhang@ybu.edu.cn

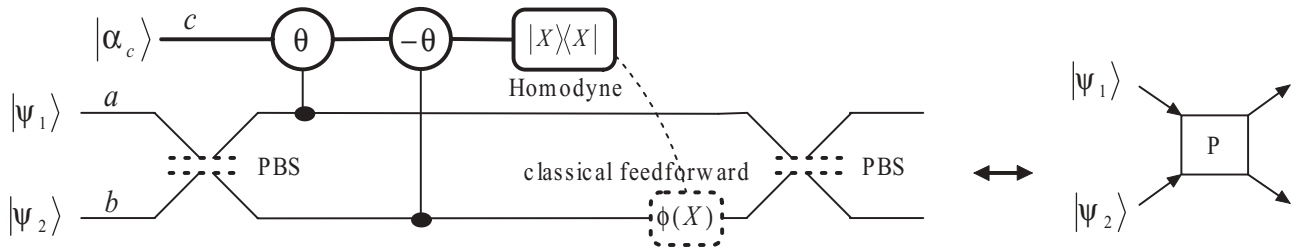

FIG. 1. (left) The parity meter for photonic qubit coding in the polarization degree of freedom. PBS indicates polarizing beam splitter. The θ indicates that the coherent beam in mode c will pick up a phase shift θ when there is a photon in mode a. $\phi(X)$ represents a phase shift dependent on the feedforward result of the homodyne measurement. (right) The circuit shown to the left.

$|\psi_{12\alpha_c}\rangle$ onto the eigenstate $|x\rangle$ of the observable X,

$$|\tilde{\psi}_{12\alpha_c}\rangle = \langle x|\psi_{12\alpha_c}\rangle = f(x,\alpha_c)(\alpha\delta|HH\rangle + \beta\gamma|VV\rangle) + f(x,\alpha_c\cos 2\theta)(e^{-i\phi(x)}\alpha\gamma|HV\rangle + e^{i\phi(x)}\beta\delta|VH\rangle), \tag{3}$$

where

$$f(x,\xi) \equiv \frac{1}{\sqrt[4]{2\pi}}\exp\left[-\frac{1}{4}(x-2\xi)^2\right], \quad \phi(x) \equiv \alpha_c \sin 2\theta(x - 2\alpha_c\cos 2\theta) \bmod 2\pi. \tag{4}$$

Here $f(x,\alpha_c)$ and $f(x,\alpha_c\cos 2\theta)$ are Gaussian probability amplitudes of the two states $\alpha\delta|HH\rangle + \beta\gamma|VV\rangle$ and $e^{-i\phi(x)}\alpha\gamma|HV\rangle + e^{i\phi(x)}\beta\delta|VH\rangle$, respectively. Therefore, the two Gaussian curves with two peaks located at $2\alpha_c$ and $2\alpha_c\cos 2\theta$ (as shown in Fig. 2) correspond to different qubit parities. The only difference between our scheme and that of Ref. [23] is that we double the θ in Ref. [23], which makes our scheme have less error probability, as described below.

The error probability can be obtained with the same method as in Ref. [22]. The small overlap between the two Gaussian curves amounts to the error probability, which is given by $P_{\text{error}} = \frac{1}{2}\text{erfc}(x_d/2\sqrt{2})$, where $x_d = 2\alpha_c(1-\cos 2\theta)$ is the distance between two peaks. As $\theta \ll \pi$ for the regime of weak cross-Kerr nonlinearities, $x_d \sim 4\alpha_c\theta^2$. Hence, comparing our scheme with that in Ref. [23], the error probability of the former $P_{\text{error}} = \frac{1}{2}\text{erfc}(\sqrt{2}\alpha_c\theta^2)$, while in the latter $P'_{\text{error}} = \frac{1}{2}\text{erfc}(\alpha_c\theta^2/2\sqrt{2})$. If we choose the same coherent probe beam and weak cross-Kerr nonlinearities as the latter, i.e., $\alpha_c\theta^2 > 9$, P_{error} is less than 10^{-12}, while P'_{error} is less than 10^{-5}. On the other hand, if we have the same error probability and coherent probe beam as in Ref. [23], the phase shift required in our scheme reduces to half, which will be more feasible in the experiment with weak cross-Kerr nonlinearities.

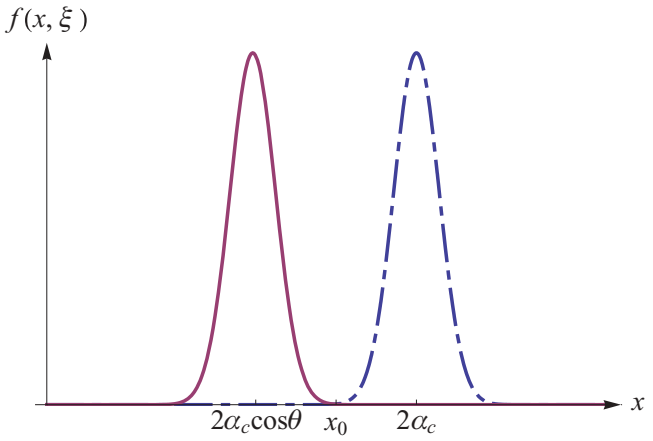

FIG. 2. (Color online) Gaussian probability distribution for the result of the X-quadrature homodyne measurement. The dashed curve and the solid curve correspond to $f(x,\alpha_c)$ and $f(x,\alpha_c\cos 2\theta)$, respectively. x_0 is the midpoint between two peaks.

Now we discuss how to generate cluster states with the parity meter proposed above. As shown in Fig. 3(a), let two photons 1 and 2 prepared initially with $|\psi_{12}\rangle = |+\rangle_1 \otimes |+\rangle_2$ simultaneously impinge on the parity meter from different arms, where $|+\rangle_i = \frac{1}{\sqrt{2}}(|H\rangle_i + |V\rangle_i)$. When $P = 0$, the initial state will collapse to $|\psi^0_{12}\rangle = \frac{1}{\sqrt{2}}(|HH\rangle + |VV\rangle)$, and we choose $\sigma = I$. Then, let the second photon through a half-wave plate (HWP) set at 22.5° (this value will be used throughout), which is equivalent to a Hadamard rotation:

$$|H\rangle \to \tfrac{1}{\sqrt{2}}(|H\rangle + |V\rangle), \quad |V\rangle \to \tfrac{1}{\sqrt{2}}(|H\rangle - |V\rangle). \tag{5}$$

$|\psi^0_{12}\rangle$ will become

$$|\psi^{0'}_{12}\rangle = \tfrac{1}{2}(|HH\rangle + |HV\rangle + |VH\rangle - |VV\rangle). \tag{6}$$

When $P = 1$, we can obtain the same result as in Eq. (6) with $\sigma = \sigma_x$, where σ_x is Pauli X operator. It is evident that Fig. 3(a) is an encoder for transforming the product state $|+\rangle_1 \otimes |+\rangle_2$ to the entangled state shown as Eq. (6).

Straightforwardly, an N-particle cluster state can be generated using the N encoders proposed above in series, as shown in Fig. 3(b). The operator σ_i depends on P_i. $\sigma_i = I$ for $P_i = 0$, and $\sigma_i = \sigma_x$ for $P_i = 1$. Consider N photons prepared initially in a product state,

$$|\phi_0\rangle = \otimes_{i=1}^{N}|+\rangle_i, \tag{7}$$

to illustrate the process for generating cluster states, where i stands for the ith photon. By a simple calculation, we find that, when $P_1 = P_2 = \cdots = P_N = 0$, the output state becomes

$$|\phi_0\rangle = \frac{1}{\sqrt{2^N}}\otimes_{i=1}^{N}\left(|H\rangle_i + |V\rangle_i\sigma_z^{i+1}\right), \tag{8}$$

where σ_z is a Pauli Z operator and $\sigma_z^{N+1} = I$. Equation (8) is a standard form of cluster state. When $P_i = 1$, we can obtain the same result as in Eq. (8) by choosing $\sigma_i = \sigma_x$. Because the error probability of a parity meter $P_{\text{error}} < 10^{-12}$, the failure probability of generating an N-particle cluster state is

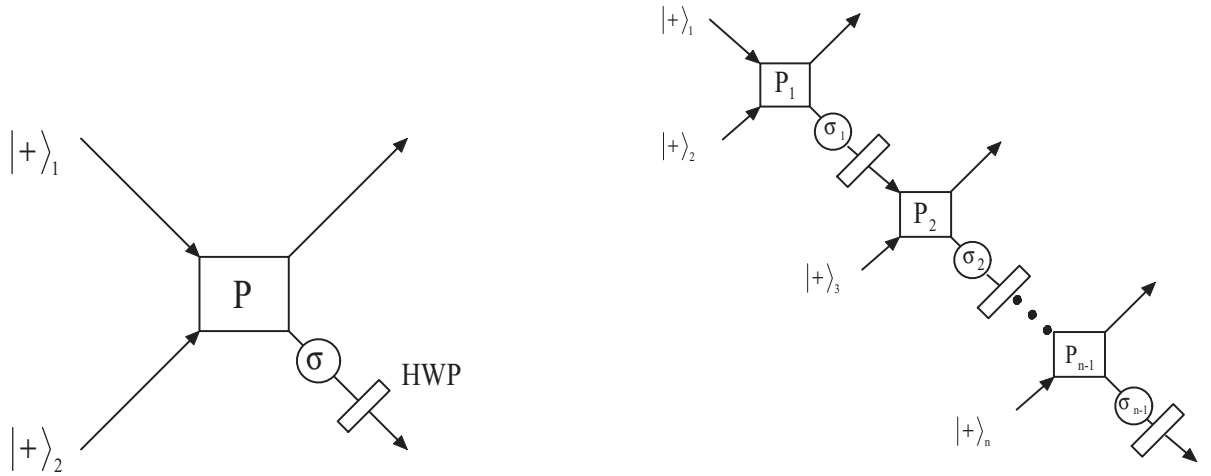

(a) (b)

FIG. 3. (a) An encoder for transforming the product state $|+\rangle_1 \otimes |+\rangle_2$ to the entangled state $\frac{1}{2}(|HH\rangle + |HV\rangle + |VH\rangle - |VV\rangle)$. The block P is the parity meter shown in Fig. 1. σ is dependent on the result of the parity meter, $\sigma = I$ for $P = 0$ and $\sigma = \sigma_x$ for $P = 1$. HWP is a half-wave plate oriented at 22.5°. (b) The setup for generating an N-particle cluster state, which is N encoders shown in Fig. 3(a) in series.

$(N-1)P_{\text{error}}$. That is, when N is not very large, the generation is also nearly deterministic. In addition, Fig. 3(a) can be used as the gate to make an N-particle cluster state and a state $|+\rangle$ fuse to an $(N+1)$-particle cluster state.

In what follows, we will construct a BSA and teleport an arbitrary unknown state with the present parity meter. The device in the rounded rectangle in Fig. 4 is the present BSA, which is composed by two parity meters and four HWPs. After the first parity meter, the Bell states in the polarization degree of freedom $|\phi^{\pm}\rangle = \frac{1}{\sqrt{2}}(|HH\rangle \pm |VV\rangle)$ can be distinguished from $|\psi^{\pm}\rangle = \frac{1}{\sqrt{2}}(|HV\rangle \pm |VH\rangle)$. Then, we perform bilateral Hadamard rotations of both photons in a Bell state, which leave the states $|\phi^+\rangle$ and $|\psi^-\rangle$ invariant, interchanging the states $|\phi^-\rangle$ and $|\psi^+\rangle$. So after the second parity meter, we can distinguish $|\psi^+\rangle$, $|\phi^+\rangle$ from $|\psi^-\rangle$, $|\phi^-\rangle$. Hence, the four Bell states can be completely distinguished. Compared with that in Ref. [28], the present BSA does not destroy the measured state. Therefore, the BSA is nearly deterministic and nondestructive.

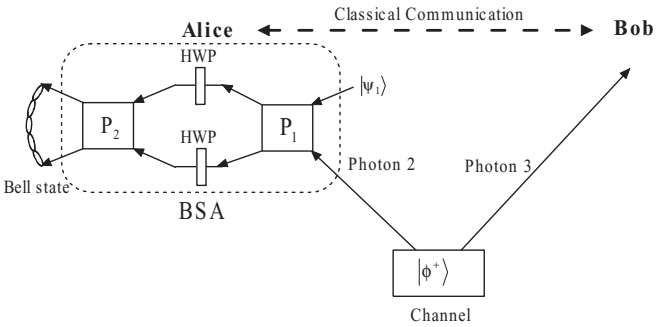

FIG. 4. Diagrammatic illustration of quantum teleportation. $|\phi^+\rangle = \frac{1}{\sqrt{2}}(|HH\rangle + |VV\rangle)$ is shared by Alice and Bob. The blocks P_1 and P_2 are the parity meters shown in Fig. 1. The device in the rounded rectangle is the present BSA. The cross curve at the left of Alice indicates that Alice will obtain one Bell state after quantum teleportation.

Using the present BSA, we can teleport an arbitrary unknown state. Suppose Alice wants to teleport an arbitrary state $|\psi_1\rangle = \alpha|H\rangle + \beta|V\rangle$ with $|\alpha|^2 + |\beta|^2 = 1$ to Bob, who is in a distant location. Choose the Bell state $|\phi^+_{23}\rangle = \frac{1}{\sqrt{2}}(|HH\rangle + |VV\rangle)$ as the entanglement channel. Photons 1 and 2 belong to Alice, and photon 3 belongs to Bob. Alice performs a Bell-state analysis on photons 1 and 2 (see Fig. 4). Then, Alice tells her result to Bob with classical communication, and Bob can recover the teleported state $|\psi_1\rangle$ by performing appropriate local single-qubit operations on photon 3 according to Alice's result. We can see the present quantum teleportation scheme is nearly deterministic due to the nearly deterministic BSA. In addition, it is worth mentioning that Alice will obtain a maximum Bell state after the teleportation, which is a by-product of the teleportation scheme and can be used for other QIP.

So far, we have shown a simplified parity meter for photonic qubits and discussed its applications in cluster-state generation, complete BSA, and quantum teleportation. One can see that the main idea in this Brief Report is also based on quantum nondemolition measurement of the photon number via cross-Kerr nonlinearity. The error probability of the present parity meter P_{error} equals $\frac{1}{2}\text{erfc}(\sqrt{2}\alpha_c\theta^2)$, which decreases as $\alpha\theta^2$ increases. Therefore, the amplitude of the coherent state and the property of the nonlinear cross-Kerr material jointly determine the success probability of our schemes. In practice, strong Kerr nonlinearities are not available in current technology; hence, we need to choose strong amplitude coherent states to decrease the error probability. A suitable Kerr nonlinear media can be provided by a two-dimensional photonic crystal waveguide constructed from diamond thin film with nitrogen-vacancy color centers fabricated in the center of the waveguide channel [29,30]. Moreover, in 2003, Hofmann *et al.* [31] showed that a phase shift of π can be

achieved with a single two-level atom in a one-sided cavity. That is to say, the present protocols are feasible and nearly deterministic, as previously mentioned.

However, it should be noted that the above analysis is carried out under ideal conditions, which is impractical in actual experiments. Many factors will affect the experimental performance, such as dispersion, self-phase modulation (SPM), molecular vibrations in Kerr media, etc. Shapiro *et al.* [32] analyzed in detail phase noise and its effect on the parity meter of Ref. [25], using the continuous-time model for cross-phase modulation. SPM can be suppressed by operating in the slow-response regime, so phase noise is caused mainly by coupling to localized noise oscillators. Their analysis showed that phase-noise terms will preclude satisfactory performance of the parity meter in Ref. [25]; for optimum performance, the following three conditions must be satisfied simultaneously:

$$\theta^2|\alpha_c|^2 \gg 1, \quad \sigma^2|\alpha_c|^2 \ll 1, \quad \sigma^2 \ll 1, \tag{9}$$

where σ^2 is the common variance of the phase noise. This result also applies to our parity meter as we have the same number of cross-Kerr media and optical pulses as Ref. [25]. The first condition in Eq. (9) has been discussed above, while the actual requirements of the last two conditions is that σ^2 is small enough. From Fig. 3 of Ref. [32], we can see the parity meter has higher success probability when $\sigma^2 \leqslant 10^{-5}$, which is a huge challenge for the current experimental conditions.

In summary, we have proposed a simplified parity meter with cross-Kerr nonlinearities and homodyne measurement. Our scheme has lower error probability and can be achieved with weaker cross-Kerr nonlinearities than the existing protocol. Furthermore, we have discussed the applications of the present parity meter in the optical QIP from three aspects: cluster-state preparation, Bell-state analysis, and deterministic quantum teleportation. All of these schemes are nearly deterministic in the regime of little noise and may be useful to future optical QIP.

This work is supported by the National Natural Science Foundation of China under Grants No. 61068001 and No. 11064016.

[1] A. Imamoğlu, D. D. Awschalom, G. Burkard, D. P. DiVincenzo, D. Loss, M. Sherwin, and A. Small, Phys. Rev. Lett. **83**, 4204 (1999).
[2] S. B. Zheng and G. C. Guo, Phys. Rev. Lett. **85**, 2392 (2000).
[3] D. Kielpinski, C. Monroe, and D. J. Wineland, Nature (London) **417**, 709 (2002).
[4] A. Steane, C. F. Roos, D. Stevens, A. Mundt, D. Leibfried, F. Schmidt-Kaler, and R. Blatt, Phys. Rev. A **62**, 042305 (2000).
[5] D. Loss and D. P. DiVincenzo, Phys. Rev. A **57**, 120 (1998).
[6] M. Bayer, P. Hawrylak, K. Hinzer, S. Fafard, M. Korkusinski, Z. R. Wasilewski, O. Stern, and A. Forchel, Science **291**, 5503 (2001).
[7] J. Q. You and F. Nori, Phys. Rev. B **68**, 064509 (2003).
[8] Z. R. Lin, G. P. Guo, T. Tu, F. Y. Zhu, and G. C. Guo, Phys. Rev. Lett. **101**, 230501 (2008).
[9] E. Knill, R. Laflamme, and G. J. Milburn, Nature (London) **409**, 46 (2001).
[10] J. W. Pan, S. Gasparoni, R. Ursin, G. Weihs, and A. Zeilinger, Nature (London) **423**, 417 (2003).
[11] R. Raussendorf, D. E. Browne, and H. J. Briegel, Phys. Rev. A **68**, 022312 (2003).
[12] P. Kok, W. J. Munro, K. Nemoto, T. C. Ralph, J. P. Dowling, and G. J. Milburn, Rev. Mod. Phys. **79**, 135 (2007).
[13] T. C. Ralph, N. K. Langford, T. B. Bell, and A. G. White, Phys. Rev. A **65**, 062324 (2002).
[14] C. W. J. Beenakker, D. P. DiVincenzo, C. Emary, and M. Kindermann, Phys. Rev. Lett. **93**, 020501 (2004).
[15] H. A. Engel and D. Loss, Science **309**, 586 (2005).
[16] B. Trauzettel, A. N. Jordan, C. W. J. Beenakker, and M. Büttiker, Phys. Rev. B **73**, 235331 (2006).
[17] O. Zilberberg, B. Braunecker, and D. Loss, Phys. Rev. A **77**, 012327 (2008).
[18] X. L. Feng, L. C. Kwek, and C. H. Oh, Phys. Rev. A **71**, 064301 (2005).
[19] X. L. Zhang, M. Feng, and K. L. Gao, Phys. Rev. A **73**, 014301 (2006).
[20] A. I. Signal and U. Zülicke, Appl. Phys. Lett. **87**, 102102 (2005).
[21] W. J. Munro, K. Nemoto, R. G. Beausoleil, and T. P. Spiller, Phys. Rev. A **71**, 033819 (2005).
[22] S. D. Barrett, P. Kok, K. Nemoto, R. G. Beausoleil, W. J. Munro, and T. P. Spiller, Phys. Rev. A **71**, 060302 (2005).
[23] K. Nemoto and W. J. Munro, Phys. Rev. Lett. **93**, 250502 (2004).
[24] W. J. Munro, K. Nemoto, T. P. Spiller, S. D. Barrett, P. Kok, and R. G. Beausoleil, J. Opt. B: Quantum Semiclassical Opt. **7**, S135 (2005).
[25] W. J. Munro, K. Nemoto, and T. P. Spiller, New J. Phys. **7**, 137 (2005).
[26] P. Kok, Phys. Rev. A **77**, 013808 (2008).
[27] X. D. Yang, S. J. Li, C. H. Zhang, and H. Wang, J. Opt. Soc. Am. B **26**, 1423 (2009).
[28] Y. B. Sheng, F. G. Deng, and G. L. Long, Phys. Rev. A **82**, 032318 (2010).
[29] P. R. Hemmer, A. V. Turukhin, M. S. Shahriar, and J. A. Musser, Opt. Lett. **26**, 361 (2001).
[30] M. S. Shahriar, P. R. Hemmer, S. Lloyd, P. S. Bhatia, and A. E. Craig, Phys. Rev. A **66**, 032301 (2002).
[31] H. F. Hofmann, K. Kojima, S. Takeuchi, and K. Sasaki, J. Opt. B: Quantum Semiclassical Opt. **5**, 218 (2003).
[32] J. H. Shapiro and M. Razavi, New J. Phys. **9**, 16 (2007).